Vincent Kotzsch

On Multi-User Transmission in Asynchronous Cooperating Base Station Systems - Theory and Practical Verification

Beiträge aus der Informationstechnik

Mobile Nachrichtenübertragung
Nr. 60

Vincent Kotzsch

On Multi-User Transmission in Asynchronous Cooperating Base Station Systems - Theory and Practical Verification

VOGT

Dresden 2012

Bibliografische Information der Deutschen Bibliothek
Die Deutsche Bibliothek verzeichnet diese Publikation in der Deutschen Nationalbibliografie; detaillierte bibliografische Daten sind im Internet über http://dnb.ddb.de abrufbar.

Bibliographic Information published by the Deutsche Bibliothek
The Deutsche Bibliothek lists this publication in the Deutsche Nationalbibliografie; detailed bibiograpic data is available in the internet at http://dnb.ddb.de.

Zugl.: Dresden, Techn. Univ., Diss., 2012

Die vorliegende Arbeit stimmt mit dem Original der Dissertation „On Multi-User Transmission in Asynchronous Cooperating Base Station Systems - Theory and Practical Verification“ von Vincent Kotzsch überein.

Gesetzt vom Autor

ISBN 978-3-938860-53-3

Jörg Vogt Verlag
Niederwaldstr. 36
01277 Dresden
Germany

Phone: +49-(0)351-31403921
Telefax: +49-(0)351-31403918
e-mail: info@vogtverlag.de
Internet : www.vogtverlag.de

Technische Universität Dresden

On Multi-User Transmission in Asynchronous Cooperating Base Station Systems - Theory and Practical Verification -

Vincent Kotzsch

der Fakultät Elektrotechnik und Informationstechnik
der Technischen Universität Dresden

zur Erlangung des akademischen Grades eines

Doktoringenieurs

(Dr.-Ing.)

genehmigte Dissertation

Vorsitzender:	Prof. Dr.-Ing. habil. Leon Urbas
Gutachter:	Prof. Dr.-Ing. Dr. h.c. Gerhard Fettweis
	Prof. Dr.-Ing. Armin Dekorsy
Tag der Einreichung:	02. Juli 2012
Tag der Verteidigung:	01. Oktober 2012

ABSTRACT

This thesis investigates techniques of multi-user communication in asynchronous transmission systems. This mainly concerns asynchronisms in time and frequency which occur in cellular wireless communication systems where multiple base stations jointly serve clusters of users which transmit on same time and frequency resources. Based on a general timing analysis on system level it is shown that particularly for large inter-site distances the unavoidable time differences of arrival severely decrease the system performance. In order to provide an in-depth analysis of the occurring asynchronous interference power the conventional MIMO-OFDM transmission model in frequency domain is extended including the combined effects of time and frequency asynchronisms. In addition to spatial multi-user interference in such systems the receiver has also to cope with inter-carrier and inter-symbol interference. Therefore, the derived frequency domain transmission model is used to accurately describe the couplings among consecutive OFDM symbols and adjacent subcarriers.

Based on this analysis techniques of linear interference suppression as well as non-linear interference cancellation are proposed. All algorithms are examined in terms of their implementation complexity. It is shown that the specific structure of the asynchronous interference power distribution across the subcarriers can efficiently be exploited to reduce the implementation complexity of the suggested algorithms. In order to show if the predicted performance gains are also observable in practical measurements, at first estimation algorithms are derived for providing the required parameter knowledge. After investigating the algorithm performance with imperfect channel knowledge, results of practical measurements in a laboratory environment are discussed. With these measurements it is verified that the derived coupling models are applicable to real transmission channels as well as that the expected performance improvements of the asynchronous interference suppression and cancellation algorithms are also visible when using practical hardware systems.

KURZFASSUNG

Die vorliegende Arbeit dient der Untersuchung von Techniken zur Mehrnutzerkommunikation in asynchronen Übertragungssystemen. Dies beinhaltet die auftretenden Effekte von Zeit- und Frequenz-Asynchronitäten, wie sie in zellularen drahtlosen Kommunikationssystemen zu beobachten sind, in welchen mehrere Basisstationen gemeinsam Nutzer versorgen, welche dieselben Zeit- und Frequenzressourcen belegen. Basierend auf einer Analyse der auftretenden Zeitversätze in solchen Systemen, wird gezeigt, dass diese insbesondere bei großen Basisstationsabständen zu erheblichen Einbußen bezüglich der Systemleistung führen. Um eine Untersuchung der zu erwartenden Interferenzleistungen zu ermöglichen, wird ein MIMO-OFDM Übertragungsmodell in der Frequenzdomäne abgeleitet, welches die Effekte der Zeit- und Frequenz-Asynchronitäten entsprechend abbildet. Zusätzlich zur räumlichen Mehrnutzerinterferenz müssen nun im Empfänger ebenso Interträger- sowie Intersymbolinterferenz berücksichtigt werden. Hierbei dient das erweiterte Übertragungsmodell für die korrekte Beschreibung der Verkopplung von aufeinanderfolgenden OFDM Symbolen und benachbarten Unterträgern.

Basierend auf diesen Zusammenhängen werden Algorithmen für die lineare Interferenzunterdrückung sowie die nichtlineare Interferenzreduktion vorgeschlagen. Die spezifische Struktur der Verteilung der asynchronen Interferenzleistung über die Unterträger ist für eine effiziente Komplexitätsreduktion der untersuchten Algorithmen ausnutzbar. Um zu zeigen dass die Kompensationsalgorithmen auch in praktischen Systemen zu den gezeigten Gewinnen führen, werden Schätzalgorithmen abgeleitet, welche die benötigte Kanalkenntnis bereitstellen. Nach Untersuchung der Leistungsfähigkeit der vorgeschlagenen Algorithmen mit imperfekter Kanalkenntnis, werden anschließend Resultate von praktischen Labormessungen diskutiert. Ziel dieser Messungen ist zu zeigen, dass die vorgestellten Kopplungsmodelle auch auf reale Übertragungskanäle anwendbar sind sowie dass die prädizierten Leistungsgewinne auch bei Nutzung herkömmlicher Übertragungstechnik den Beobachtungen entsprechen.

ACKNOWLEDGEMENT

This thesis is the result of my work at the Vodafone Chair Mobile Communication Systems at Technische Universität Dresden from 2008 to 2012. I want particularly express my gratitude to Professor Gerhard Fettweis who not only gave me the opportunity to work at such an excellent and exciting place like the Vodafone Chair but also significantly contributed to improve my personal and professional skills. Working with so much smart persons on national and international level definitely inspired me and broadened my understanding of research.

The results of my scientific work at the chair are part of this thesis. The final version of this thesis would not have been possible without the support of Dr. Wolfgang Rave, Jörg Holfeld and Hans-Christoph Kotzsch. Their valuable comments and corrections helped to improve the work significantly. Moreover, I would like also express gratefulness to Professor Armin Dekorsy for acting as referee for this thesis.

My career in wireless communications started in 2004 at the company Signalion which was founded by former PhD graduates of the Vodafone chair. The work there gave me valuable insights into numerous issues that must be considered when developing radio systems. After finished my master thesis, I was really happy to got the chance to extend my knowledge and continuing the scientific work as a research associate at the university. Together with Signalion in the EASY-C project we developed one of the first demonstrators for testing coordinated multi-point systems in practical field trials. One problem that arises in such systems is the network synchronization which was the initial motivation for covering this topic in my thesis.

My career as researcher started in the signal processing group of the chair which is headed by Dr. Wolfgang Rave. His valuable guidance and supervision has gained my sensitivity when developing new ideas to meaningful scientific results. But also the discussions with the other group members Jörg Holfeld, Stefan Wesemann and Patrick Grosa led to a better understanding of many problems. Furthermore, countless talks with chair members like Eckhard Ohlmer, Albrecht Fehske, Fabian Diehm, Michael Grieger, Ines Riedel, Vinay Suryaprakash and others helped me to refine my basic ideas as well as to focus the work on the actual key issues.

Moreover, without the substantial help of Ainoa Navarro Caldevilla and Sven-Einar Breuer during the lab trials many of the measurement results were not part of this thesis. A special thanks also to Dr. Patrick Marsch who originally motivated me to join the chair as well as to be a part of the great EASY-C team.

Without doubts doing research is very fascinating but particularly if nothing happens as expected it is wonderful to relax with friends gathering new energy and getting ideas for solving remaining problems. Therefore, I would like to thank all of my friends with whom I did many exciting things besides work. Moreover, I would like to thank my large family for constantly supporting me during the last years.

Dresden, 01.07.2012 Vincent Kotzsch

CONTENTS

CHAPTER 1

INTRODUCTION

COMMUNICATION systems in the physical sense are defined by transmitting any type of information between separated sources and sinks by using an electromagnetic system. Early principles of *wired* electric communication already were investigated in the first half of the 19th century and Samuel F. B. Morse first patented an electric telegraph in 1840[1]. Influenced by groundbreaking new results in the field of electromagnetism and wave theory by James C. Maxwell and Heinrich Hertz in 1864 and 1888 respectively, in 1896 Guglielmo Marconi has patented a complete apparatus for *wireless* communication. Communication in the early years mainly meant to transmit electric impulses via telegraphs. The first communication device with speech transmission was presented by Philipp Reis in 1861 and was named telephone. The first person who have carried out a wireless speech transmission was Reginald Fessenden who broadcasted a live radio stream on christmas in 1906. The breakthrough for wireless telephony was possible after Lee De Forest invented the Audion in 1906 which could be used to generate and amplify radio signals and so enabled the transmission over long distances. After decades of vast innovations in the field of wireless communications, including e.g. radio and television, the first principles of cellular wireless communication networks were discussed around 1979.

Due to the technical advantages in the computer science the devices became smaller and also usable as *true* mobile devices and in particular affordable. Thus, after some smaller predecessor networks in 1991 the famous GSM[2] system has been launched which is used still today. Due to the invention of the world wide web and the move from speech transmission to the transmission of packet oriented digital data a new high demand for more capacity was needed. This has been realized by the 3GPP/UMTS[3] system, driven by the 3rd generation partnership project

[1] For more details about the history of wireless communication see also [Sol99].
[2] GSM $\triangleq$ Global System for Mobile Communications, see also [Rap02].
[3] UMTS $\triangleq$ Universal Mobile Telecommunications System, see also [Rap02].

(3GPP), which however did not sustain the fast increasing requirements for a long time. The latest generation in cellular communication is known as 3GPP/Long Term Evolution (LTE) system (see also [STB09]) which aims again to exploit the available spectrum more efficiently in order to increase the data rates. To address the forecasted capacity requirements in the next years as well as the need of more flexibility in the spectrum usage, LTE Advanced is being standardized currently (see also [3GP10]). It incorporates a lot of new transmission techniques such as base station cooperation which is also referred to as coordinated multi-point (CoMP).

Cooperating base station systems in general aim at exploiting the capacity gains known from the multiple-input multiple-output (MIMO) systems also on cellular level with distributed antennas[4] in order to increase the spectral efficiency particularly at the cell edges. The gains of MIMO compared to conventional single antenna systems are achievable due to the utilization of the spatial domain in addition to the well known time and frequency domain which increases the total number of available channel resources for data transmission (see also [Fos98], [Tel99]). One main issue in cellular communication networks is the general wireless channel access of multiple users. Basically the data transmission resources can be divided into time, frequency and space. In single link systems, as e.g. GSM, the users are forced to transmit on orthogonal resources by using a time/frequency division multiplex. The space is "multiplexed" by reusing the same time/frequency resources in a certain physical distance between the transmitters where the signal attenuation, caused by the pathloss, has already decoupled the signals (see also [Rap02]). In frequency reuse one systems this is not the case so that the transmit signals are spatially superimposed. This signal coupling must be reversed at the transmitter or receiver side. In code division multiple access (CDMA) systems, like UMTS, orthogonal codes are exploited to suppress the spatial interference (see also [Ver98], [Küh06]). This technique enabled frequency reuse one systems but due to the orthogonality loss under practical conditions the capacity could not be increased significantly. In conventional MIMO systems the spatial signal coupling is reversed by exploiting techniques from classical estimation theory (see also [Say08], [Sch91]) that requires a quite large amount of additional signal processing resources.

In the existing literature the term MIMO is mainly used to express a single link point to point transmission with multiple antennas at *one* transmitter and *one* receiver station. The MIMO principle itself has already been used in cellular context as well but so far the required signal processing is restricted to be in one device. The term single user MIMO is equal to single link MIMO with multiple antennas at the base station as well as user terminals where the spatial decoupling is employed either in the base station or in the terminal. In multi-user MIMO systems (see e.g. [JH07],[GKH$^+$07]) the spatial decoupling of geographically separated users can only be accomplished within one base station with multiple antennas since the users are not able to cooperate. In virtual or network MIMO systems signal observations from more than one base station are supposed to be exploited for the spatial decoupling of the users. Network MIMO therefore represents the general class of multi-point to multi-point MIMO systems since

[4]CoMP systems are sometimes also referred to as distributed antenna systems (DAS).

it is assumed that the transmit and receive antennas are not restricted to be at the same location as it is the case for single link MIMO. Systems with explicit base station cooperation were first described in [And05] or [KFV06]. A comprehensive overview about recent achievements in CoMP systems is e.g. given in [MF11] or [GHH+10]. It should be noted that there are also other types of base station cooperation such as coordinated scheduling. The investigation of those techniques are not part of this work. In the following the terms CoMP and multi-cell network MIMO are always used equivalently.

1.1. Motivation

Although the behavior of multiple antenna systems is well known for more than a decade the transition to distributed antennas is not straightforward due to the impairments which mainly arise when moving the MIMO paradigm from point to point to multi-point to multi-point links (see e.g. [DHL+11]). In single link MIMO it is usually expected that the signal processing of the transmit signals is carried out within one device so that the signals at the output of the transmit antennas are assumed to be phase coherent. When considering multiple distinct transmitters, this assumption does not hold anymore since the transmit timing as well as the carrier frequency are not exactly aligned among the devices. Furthermore, also the radio propagation delays can differ significantly so that the signals arrive at the receivers at different time instants whichs leads to unavoidable time differences of arrival (TDOA). Although using highly efficient synchronization procedures, these impairments can lead to performance degradations in cooperating base station systems (see e.g. [ZMM+08]). Since the costs for the roll out of the CoMP technology are relatively high the question arises how much gains can be expected in impaired transmission channels and whether a joint signal processing is still beneficial compared to other transmission techniques?

In today's wireless communication systems mainly the orthogonal frequency division multiple access (OFDMA) modulation technique is employed as it provides a very flexible resource allocation and a low complexity channel equalization particularly for frequency selective channels. Unfortunately, OFDM is very sensitive to impairments of the radio link such as asynchronisms (see e.g. [SFFM99]) and thus is advantageous only in transmission channels with perfect synchronization. When considering symbol timing offsets (STO) in OFDM, a guard interval, usually designed as cyclic prefix (CP) , is used to avoid inter-symbol interference of consecutive OFDM symbols. But in cooperating base station systems one receiver can only be aligned to one transmitter. Thus, the resulting TDOA can lead to inter-symbol interference from the unaligned superimposed user when exceeding the CP limit. Clearly, the cyclic prefix leads inherently to a capacity loss. Therefore, its length is limited in order to have a good trade-off between spectral efficiency and the expected maximum timing delays. As a consequence CoMP systems are restricted to be used mainly in networks with small inter-cell distances where the possible TDOAs are assumed to be much less than the cyclic prefix length.

1.2. Related Work

The impact of time and frequency asynchronisms to OFDM systems itself is a well investigated research area in the wireless communication community. Asynchronous co-channel interference caused by the Doppler effect which is similar to a carrier frequency offset (CFO) is already investigated in [RS95]. Inter-carrier interference caused by frequency offsets and partly also its compensation is e.g. analyzed in detail in [ETWH01], [SDAD02], [IBN03], [HL05] [LLTC06], [MFP06] or [SJ09]. Thus, the impact of misaligned subcarrier frequencies on the OFDM system performance is well understood but often the analysis is only carried out on link level without considering the pathloss effects which occur on a large-scale level. The same can be studied for the case of timing errors in OFDM which are e.g. part of the investigations in [SFFM99], [NK02], [CZ04],[MC06], [HS09] or in [Ham10] as well as in [SSF03], [JZ04], [NUNH07], [HS08] or [ITKA09] with the focus on interference cancellation algorithms. The motivation for the assumption of carrier frequency offsets are mainly imperfect oscillators, the Doppler effect as well as imperfect parameter estimation. The motivation for considering symbol timing offsets are mainly long echo fading channels or small cyclic prefix lengths so that already low timing estimation errors lead to inter-symbol interference. But as e.g. summarized in [MKP07], algorithms for estimating time and frequency mismatches are well established and proved in practical systems. Therefore, it can be assumed that for single link transmissions a sufficient synchronization in time and frequency can be achieved.

As mentioned above, this is not the case for multi-point to multi-point systems. Since the impact of the occurring time and frequency offsets on the OFDM system remains the same in multi-point systems there might be users that produce *asynchronous* multi-user interference. The impact of such time asynchronisms to the multi-cell cooperation is e.g. considered in [ZMM+08] as well as in [KMG+08] with results that basically show the overall system performance. Both contributions provide a very good insight into the basic problem but unfortunately do not include a detailed interference analysis including also channel characteristics observable on system level. A remaining problem is therefore the combined analysis of time and frequency errors in large-scale multi-point to multi-point MIMO OFDM networks and its compensation.

1.3. Contribution of the Thesis

As it can be concluded from the above remarks, so far the impact of asynchronisms in OFDM based CoMP systems on a large-scale level is not well investigated, since usually the guard interval is assumed to be long enough and the frequencies are assumed to be perfectly aligned. This simplifies the performance analysis a lot but does not reflect the real system behavior. Three remaining questions related to the impact of asynchronisms in OFDM based CoMP are:

- How large is the asynchronous interference in general when considering CFOs and TDOAs coupled with the pathloss and which size must the CP have to avoid inter-symbol interference that leads to a significant performance degradation?

- What are the possibilities to compensate the performance loss caused by the asynchronisms, e.g. to avoid large CP lengths, and what is about its approximate implementation complexity?
- Are the extended interference models also applicable to practical transmission systems so that numerical simulation results can be used for a reliable performance prediction?

This thesis aims at providing answers to these questions. This includes a characterization of the additional distortions caused by the asynchronisms as well as an analysis of its implication to limitations and requirements for using CoMP also in large-scale networks. The main contributions provided by this thesis can be summarized as:

- Analysis of occurring CFOs and TDOAs in cellular wireless communication networks with base station cooperation.
- Derivation of an accurate analytical frequency domain transmission model for OFDM based CoMP systems with arbitrary TDOAs and carrier frequency offsets as well as channel lengths.
- Characterization of the impact of asynchronous interference in CoMP systems on a cellular level by including also pathloss effects.
- Derivation of potential asynchronous interference cancellation and suppression methods and analysis of their applicability in a 3GPP/LTE based CoMP system.
- Investigations on parameter estimators under the impact of asynchronisms and the characterization of imperfect parameter knowledge on compensation algorithms.
- Comparison of simulation results with real world measurements in a practical 2×2 CoMP transmission scenario.

The main goal of this work is to extend the existing knowledge of OFDM based CoMP systems and provide solutions to design more robust wireless communication networks that can cope with time and frequency asynchronisms. From a system level viewpoint the introduced metrics can be used to assess for which network parameters the asynchronous multi-user interference will be the limiting factor when using CoMP. Furthermore, based on the link level analysis device manufacturers are able to design base stations that can compensate the additional asynchronous interference. In principle, both results can be exploited to increase the spectral efficiency in cooperating base stations systems.

1.4. Thesis Outline

Within the subsequent chapter 2 the basic principles of wireless communication systems are briefly reviewed. The main focus are the fundamental differences between cooperating and non-cooperating base stations systems. This includes particularly the channel coupling characteristics as well as the system limitations. The provided analysis serves as basis to proceed with chapter 3 in which the impact of the asynchronisms on the MIMO OFDM transmission is analyzed in detail. This incorporates the derivation of a convenient transmission model in frequency domain as well as an analysis of the asynchronous interference power on link level and on system level. The introduced transmission model, including all types of impairments caused by asynchronisms, is then used in chapter 4 to discuss techniques of asynchronous interference cancellation and suppression. For each of the proposed algorithms a complexity analysis is provided. In chapter 5 algorithms are introduced that are usable for obtaining the required parameter knowledge in a 3GPP/LTE system. Furthermore, the performance results obtained for the asynchronous interference cancellation and suppression algorithms in chapter 4 are evaluated with imperfect parameter knowledge. Thereafter, the key findings of the theoretic part of the thesis are proved in an exemplary 2×2 laboratory transmission setup. At the end a summary of the main results of the thesis as well as conclusions are given in chapter 6.

If the reader is not familiar with the already known fundamental results of system theory including estimation and detection theory as well as communication and information theory, it is recommended to read appendix B before starting with chapter 2. Furthermore, in appendix A the basic mathematic relations are introduced which are useful to know for reproducing the main ideas and analytical derivations.

Comments on Notation: The general definitions of the used notation as well as variables are stated in detail on pages 201-204. The most important ones are briefly introduced here as a basic starting point. In order to account for the established notation of time and frequency domain used in OFDM the transform domain variables are distinguished by lower as well as uppercase letters, e.g. x for time and X for frequency domain *signal* variables. Matrices, vectors and scalars are distinguished as boldface, underlined and plain letters, e.g. $\boldsymbol{x}$, $\underline{x}$ and x. As many components in the wireless channel communication exhibit a stochastic behavior non-italic sans-serif letters denote random variables and italic serif letters deterministic variables respectively, e.g. x and x. Functions are always indicated as normal text with their argument in curved brackets, e.g. $\log\{x\}$.

CHAPTER 2

FUNDAMENTALS OF CELLULAR WIRELESS COMMUNICATION

This chapter is intended to review the basics of cellular wireless communication with the focus on coordinated multi-point systems. A more detailed analysis of important results from communication and information theory which are used as underlying model throughout this thesis is given in appendix B.2 and the references therein. Although the system level analysis is only one small part of this thesis the knowledge of important concepts are required for the analysis on link level[1]. This concerns in particular the strong connection between the signal timing delays with the corresponding pathloss attenuations which are rather phenomena that can be observed on system level but is indispensable for understanding the impact of timing delays on the network performance. Therefore, in the first section 2.1 a review of communication systems is presented where the focus is on general transmission concepts as well as on multi-antenna multi-carrier systems. Its application to cooperating base station systems is then part of the analysis in section 2.2 where the focus is on the main network design parameters which affects the transmission performance, e.g. the link separation and the occurring synchronization inaccuracies in such types of systems. At the end a short summary of this chapter is provided. It should be noted that the important stochastic wireless channel model used as underlying model throughout this thesis is not part of this chapter but is described in detail in appendix B.3.

[1]The link level layer is also known as physical layer.

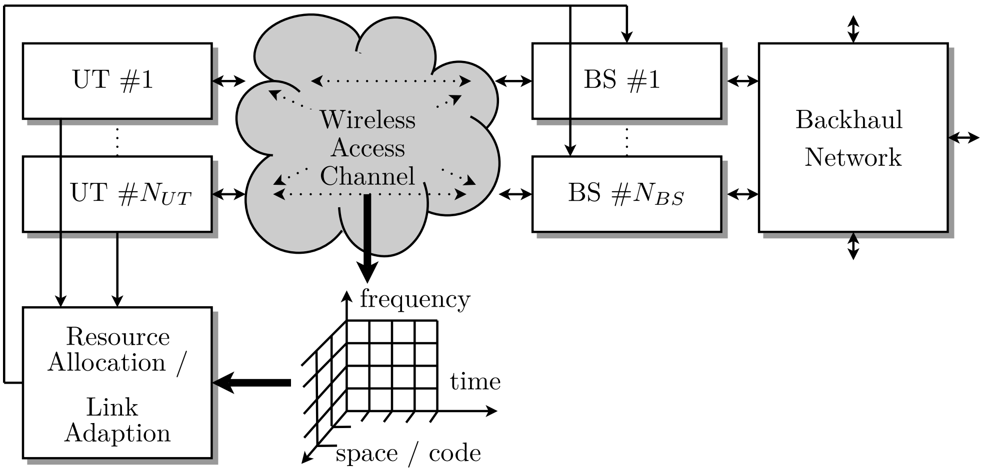

Figure 2.1.: Uplink / downlink transceiver model and multiple channel access

2.1. Review of Communication Systems

Within the past century a lot of progress has been made in communication theory. In particular the invention of information theory by Shannon in 1948 was a huge milestone. Within this section only a few small parts of communication theory important for this work are briefly introduced in the following. A comprehensive overview about cellular wireless communications as well as mobile radio propagation in general is for example given in [Rap02]. Furthermore, a detailed discussion of wireless communication principles such as digital communication can be found in [Gol05] or [Kam08]. The basic requirements of LTE systems which is used as underlying model throughout this thesis can be studied in [STB09]. Moreover, the main reference for CoMP system specifications as well as baseline references is [MF11].

2.1.1. Wireless Channel Access

The general transceiver block diagram used as underlying model throughout this work is depicted in Fig. 2.1. It is always assumed that N_{UT} active user terminals (UT) require the channel for an uplink (UL) or downlink (DL) transmission. The channel access as well as the connection to the backhaul core network is always coordinated by N_{BS} active base stations (BS)[2]. The channel access includes particularly the assignment of the available channel resources in time, frequency as well as the space dimension and the corresponding adaption of the transmission parameters in order to achieve a required link performance. Throughout this thesis only the uplink direction from the user terminals to the base stations is considered. Basically, the results introduced and discussed in this work are also applicable to the downlink direction. Therefore, in the following it is always assumed that there are K channel inputs and M channel outputs.

[2]In LTE systems the base stations are also referred to as eNB.

Interference Channel: As it is widely known since the available spectrum for signal transmission is usually scarce the signal bandwidth B_S and so the maximum throughput is limited. When considering the single link transmission model $y = hx+v$ with x as a transmit signal with a given bandwidth B_S. The (complex) multiplicative wireless channel gain h includes effects of the transmission channel between the transmit and receive antenna[3]. The variable v represents an additive distortion caused by thermal noise with the power given by the two-sided noise power spectral density[4] denoted with N_0. The single link capacity for this model is bounded by the Shannon limit with[5]:

$$\frac{C}{[\text{bit/s}]} = B_S \text{ld}\left\{1 + |h|^2 P_{max}/(N_0 B_S)\right\} \tag{2.1.1}$$

The maximum transmit power constraint which is usually defined by the governmental regulatory agency is defined by $P_{max} = \mathrm{E}\left\{|x|^2\right\}$. As it can be observed, the capacity depends mainly on the ratio between the antenna input power at the receiver and the noise power which is also referred to as signal-to-noise ratio (SNR). Therefore, the system performance can only be increased if either the bandwidth or the transmit power is increased as well. Both options are basically not easily feasible in practical deployments. In Eq. (2.1.1) only the time degree of freedom is exploited which is directly coupled to the signal bandwidth. Another degree of freedom is the spatial dimension. It is known that the signal attenuation on air decreases exponentially so that the same frequency can be reused if the signals are separated due the pathloss (PL). In Eq. (2.1.1) the assumption of a perfect rectangular low-pass filter holds which prevents adjacent carrier interference. This is not necessarily the case. In many transmission systems one has to cope with a variety of interferences. This is the reason why usually the wireless transmission channel is rather treated as interference channel. In the following the main types of interferences are briefly introduced which are often used in literature:

- Inter-carrier interference (ICI) denotes mainly the interference in frequency domain among adjacent carrier frequencies used for data transmission which are insufficiently filtered w.r.t. the bandwidth restriction.
- The term co-channel interference (CCI) which is sometimes also called adjacent-cell interference (ACI) is usually used to describe the spatial interference between neighboring cells that transmit on the same carrier.
- If multiple users must share the same resources one has to cope with multi-user interference (MUI) which is also known as multiple access interference (MAI). This type of interference usually occurs when the users explicitly transmit on the same time/frequency resource and interfere with each other.
- Since the transmission channel is often frequency selective the overlap between consecutive

[3]These effects are discussed in appendix B.3 in detail.
[4]See also appendix B.2.1.
[5]See appendix B.2.3 for a detailed discussion.

transmission symbols is called inter-symbol interference (ISI). If blocks of symbols overlap this is also referred to as inter-block interference (IBI).

- Within this work in chapter 3 the term asynchronous interference (AI) is introduced which mainly condenses the types of interferences which are caused by asynchronisms[6].

If K transmit symbols $\underline{x} \in \mathbb{C}^{K\times 1}$ interfere with each other, at the M channel outputs they are observable as superimposed signals. Using a coupling matrix $\boldsymbol{h} \in \mathbb{C}^{M\times K}$ which is still unspecified at this point[7] the transmission model can be expressed by $\underline{y} = \boldsymbol{h}\underline{x} + \underline{v}$. The transmit and receive signals as well as the noise are now column vectors. As shown in appendix B.2.3 the maximum sum capacity for those systems is given by the summation of independent single link channels with:

$$\frac{C_{sum}}{[\text{bit/s}]} = B_S \sum_{i=1}^{\kappa} \text{ld}\left\{1 + \frac{\lambda_i P_{max}}{N_0 B_S}\right\} \leq B_S \text{ld}\left\{1 + \frac{\sum_{i=1}^{\kappa} \lambda_i P_{max}}{N_0 B_S}\right\} \tag{2.1.2}$$

where λ_i are the non-zero eigenvalues of $\boldsymbol{h}\boldsymbol{h}^{\text{H}}$ and $\kappa = \text{rank}\left\{\boldsymbol{h}\boldsymbol{h}^{\text{H}}\right\}$. It should be noted that here it is assumed that the transmitters cannot cooperate so that they always transmit with full power. If a transmit cooperation is possible the optimal input power distribution would be given by the water-filling theorem[8]. Clearly, for K independent transmission channels with no coupling the capacity would reduce to the sum capacity of K single link channels since the singular values would equal the channel gains. The question is now what is the achievable single user performance in such interference channels if the interference should be minimized?

Multiple Channel Access Schemes: The transmission rate for one single link is still given by Eq. (2.1.1) but with an additional interference term in the denominator caused by the transmitter coupling. Thus, the Shannon limit for a single link i according to the signal-to-interference-plus-noise-ratio (SINR) could be obtained by:

$$\frac{C_i}{[\text{bit/s}]} = \beta_i \alpha_i B_S \text{ld}\left\{1 + \frac{|h_i|^2 p_i}{\sum_{k,k\neq i} |h_k|^2 p_k + \alpha_i N_0 B_S}\right\} \;\forall\; \alpha_i, \beta_i \leq 1 \;\wedge\; p_i \leq P_{max} \tag{2.1.3}$$

where k is used as interferer index. Of course, there are now several degrees of freedom that can be exploited by adjusting α_i, β_i as well as p_i for each user individually. Given an overall sum power constraint P_{max} and a maximum usable system bandwidth B_S there are different sum capacity points achievable when using different transmit strategies. In terms of the channel access it can be distinguished between:

- If the interference term should be avoided the available signal bandwidth needs to be multiplexed between the users ($\sum \alpha_i = 1$). Furthermore, via time sharing the rate can be

[6] The reason for that is to have a brief notion for a couple of different interference types which is often used in the literature for this purpose (Cf. [ZMM+08]).
[7] This could be the spatial or the frequency domain.
[8] See also appendix B.2.3.

split ($\sum \beta_i = 1$). Those techniques are known as time/ frequency division multiple access (TDMA/FDMA). By including variable power allocation into the optimization it can be shown that in general the achievable TDMA as well as FDMA capacities are equal.

- If the available signal bandwidth should be usable for all users ($\alpha_i, \beta_i = 1$) one has to cope with interference. In code division multiple access (CDMA) systems orthogonal codes are used to suppress the interference, but since the signals are spread by the codes the actual transmission bandwidth is reduced according to the spreading factor. When using spatial division multiple access (SDMA) either the CCI power $|h_k|^2$ is already attenuated by the pathloss or a successive interference cancellation could be used at the transmitter or receiver[9]. Furthermore, in SDMA as well as CDMA systems the CCI power can be controlled via the power values p_i and p_k. For instance, the power values can be adjusted so that a certain required quality of service is fulfilled for each user individually.

It should be noted that SDMA systems with cooperating base stations and a joint signal processing are equal to distributed antenna systems which are of particular interest throughout this work. Clearly, in SDMA systems with multiple spatial streams and interference cancellation the system capacity would be maximized.

Reference curves for the achievable capacity in systems with base station cooperation are provided in [Mar10] and [MF11]. In these publications also comparisons of different multiple channel access strategies can be found.

2.1.2. Multi-Carrier Multi-Antenna Transmission

As it was mentioned above, a flexible resource allocation is necessary to adapt the channel access scheme to the current channel state. A modulation scheme that fulfills these requirements is the technique of orthogonal frequency division multiplex (OFDM) with the adaptation to multi-user systems as orthogonal frequency division multiple access (OFDMA). The basic idea of OFDM is to divide a high rate single carrier system into a low rate multi-carrier system. Orthogonal multi-carrier systems itself are known since a few decades and first principles already have been discussed in [Cha66]. A few years later in [WE71] the authors described the exploitation of the discrete Fourier transform (DFT) within the general class of OFDM systems. Due to the technical advances in the last 20 years particularly the feasibility of an efficient implementation of the DFT the OFDM modulation techniques attracted a lot of attention again and can now be found in numerous wireless and wired communication standards.

A good overview about designing appropriate multi-user multi-carrier systems is given in [WG00] or [Kam08]. A comprehensive work about implementation issues connected to OFDM systems can be found in [HB08]. As mentioned earlier, the usage of multiple spatial streams

[9]This means that e.g. the each transmit signal can be decoded successively with an arbitrarily small error at the receiver and in conjunction with the channel information the already decoded data can be used to reconstruct and subtract the interference caused by this transmitter.

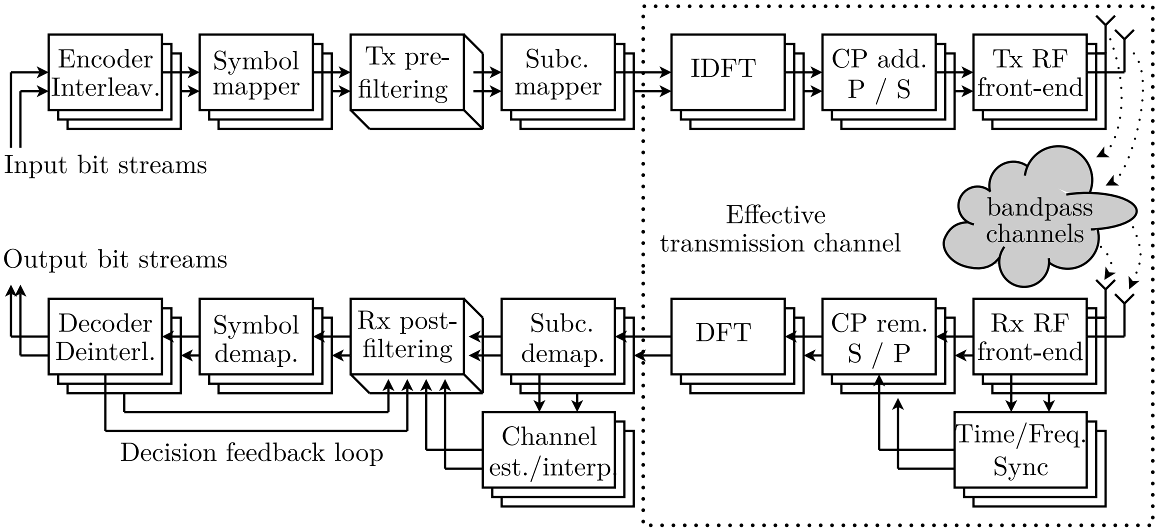

Figure 2.2.: General transceiver block diagram

promises to increase the spectral efficiency. For commercial wireless communication systems this transmission technique is only applicable since a few years due to the tremendous progress in circuit integration so that the required signal processing can be included into a single device. An overview about the feasibility of MIMO in wireless systems is e.g. given in [GSS+03], [PGNB04], [Wüb05] or in [Spe05]. Challenges for implementing a MIMO system are e.g. discussed in [SBM+04]. A good survey about the history of OFDM and MIMO as well as current state of the art multi-user MIMO OFDM transmission techniques is given in [JH07].

MIMO OFDM Transceiver Model: The basic underlying MIMO OFDM transmission model used within this work is depicted in Fig. 2.2. The starting point for deriving an analytical OFDM model is a single carrier transmission as described in appendix B.2. Assume an application that produces a continuous bit stream. The encoder block adds redundant information that can be exploited at the receiver for bit error identification as well as correction[10]. The binary input bit stream is therefore partitioned into blocks of N_I information bits with $\underline{b} \in \mathbb{F}_2^{N_I \times 1}$ which are uniquely mapped onto codewords consisting of N_C code bits $\underline{c} \in \mathbb{F}_2^{N_C \times 1}$ taken from a discrete codebook $\mathcal{C}$:

$$\underline{b} \longmapsto \underline{c} = \mathrm{enc}\{\underline{b}\} \in \mathcal{C} \tag{2.1.4}$$

The length of the codewords depends on the available resources for data transmission. For a certain code rate the corresponding length of the information bit vector is explicitly given. The interleaver permutes the codewords and is commonly followed by a bit scrambler which ensures equally probable binary values.

[10] Usually the encoder also applies a rate adaption in order to provide fractional code rates for the optimal link adaption.

Thereafter, the codewords are passed through the symbol mapper where they are partitioned into blocks of $\mathrm{ld}\,\{N_M\}$ bits. N_M denotes the modulation order here. The bit tuples are then uniquely mapped onto (complex) constellation points $X \in \mathbb{C}$ taken from a discrete symbol alphabet $\mathcal{A} \subset \mathbb{C}$:

$$\underline{c} \longmapsto X = \mathrm{mod}\{\underline{c}\} \in \mathcal{A} \tag{2.1.5}$$

In a single carrier transmission system the discrete complex transmit symbols pass through a pulse shaping filter $g(t)$ which ensures the bandwidth limitation[11]:

$$X(t) = T_{SC} \sum_{o=-\infty}^{\infty} X_o \; g_T(t - oT_{SC}) \;\; \forall \;\; t \in \mathbb{R} \tag{2.1.6}$$

where $t \in \mathbb{R}$ and $o \in \mathbb{Z}$ denote the continues as well as discrete time index, respectively. The corresponding sampling interval for one certain subcarrier is given by $T_{SC} = 1/B_{SC}$ with B_{SC} as subcarrier bandwidth. Thereafter, the continuous time signal $X(t) \in \mathbb{C}$ is up-converted to a subcarrier with frequency f_{SC}. When considering parallel carriers Eq. (2.1.6) can be rewritten to:

$$x(t) = T_{SC} \sum_{q \in \mathbb{N}} \sum_{o=-\infty}^{\infty} X_{o,q} \; g_T(t - oT_{SC}) \; e^{j2\pi f_{SC,q} t} \;\; \forall \;\; t \in \mathbb{R} \tag{2.1.7}$$

where $x(t)$ denotes the superimposed signal from all subcarriers. Throughout this thesis the variable q is used as subcarrier index. If furthermore a rectangular pulse shaping filter with:

$$g_T(t) = \begin{cases} 1/T_{SC} & 0 \le t < T_{SC} \\ 0 & \text{otherwise} \end{cases} \tag{2.1.8}$$

is assumed it holds:

$$x(t) = \sum_{q \in \mathbb{N}} X_{o,q} \; e^{j2\pi f_{SC,q} t} \;\; \forall \;\; t \in \mathbb{R} \;\; \wedge \;\; oT_{SC} \le t < (o+1)T_{SC} \tag{2.1.9}$$

The amplitude spectral density of the transmit signal is now given by the sinc spectrum. When considering Q parallel channels, with $t = nT_{SC}/Q$ and $\mathcal{Q} \subseteq \{1, \ldots, Q\}$ as well as equally spaced subcarrier distances $f_{SC,q} = q/T_{SC}$, one arrives at the well known inverse DFT (IDFT)[12]:

$$x_{o,n} = x_o(nT_{SC}/Q) = \sum_{q \in \mathcal{Q}} X_{o,q} \; e^{\frac{j2\pi qn}{Q}} \;\; \forall \;\; n \in \mathbb{Z} \;\; \wedge \;\; oQ \le n \le (o+1)Q - 1 \tag{2.1.10}$$

with $X_{o,q} = 0 \; \forall \; q \notin \mathcal{Q}$. The sinc spectrum, which is obtained when applying the discrete

[11]See also appendix B.2.1.
[12]Except the power scaling factor $1/\sqrt{Q}$.

time Fourier transform (DTFT) to $x_{o,n}$, is perfectly orthogonal among the subcarrier tones[13]. Obviously, the sampling interval of x is shortened to $T_S = T_{SC}/Q = 1/B_S$ so that there are Q samples within one *OFDM symbol*. Due to the usage of the IDFT the symbols X are usually referred to as frequency domain symbols as well as the symbols x as time domain symbols. In order to distinguish between the two domains before and after the DFT operation, throughout this thesis these definitions are used as well. For example, the variable n denotes the discrete time index in time domain while o denotes the discrete time index for one OFDM symbol. It should be noted that not all subcarriers must necessarily be used for data transmission. The indices of active subcarriers are included into the set $\mathcal{Q}$ with $N_{SC} = |\mathcal{Q}|$ which corresponds to the subcarrier mapping unit in Fig. 2.2.

As the sinc spectrum is not band-limited and thus produces out-of-band radiations, the OFDM symbols $x_{o,n}$ must be band-limited w.r.t. B_S by applying an pulse shaping filter again. Thereafter, the transmit signal is up-converted to a carrier frequency f_C. At the receiver the signal is down-converted into the baseband, sampled according to the Nyquist rate to fulfill the sampling theorem as well as quantized w.r.t. the resolution of the analog-to-digital converter (ADC). The transmission over band-limited channels is equal to the convolution with the channel impulse response (CIR) $h(t, \tau_C)$ where τ_C denotes the CIR length. For frequency selective channels with $\tau_C > 0$ it is known that the first Nyquist criterion does not hold anymore. This result is also applicable to OFDM symbols so that in the case of frequency selective channels inter-symbol interference occurs which destroys the orthogonality among the symbols. Therefore, in OFDM a guard interval in terms of a cyclic extension is preceded that should avoid the ISI[14]. For this reason Eq. (2.1.10) needs to be rewritten to:

$$x_{o,n} = x_o(nT_S) = \sum_{q\in\mathcal{Q}} X_{o,q}\, e^{\frac{j2\pi qn}{Q}} \quad \forall \;\; n \in \mathcal{N} \tag{2.1.11}$$

with $\mathcal{N} = \{n \in \mathbb{Z}| - N_{CP} + oN_O \leq n \leq (Q-1) + oN_O\}$. The length of the cyclic prefix (CP) is defined by N_{CP}. The OFDM block length, including the core symbol and the cyclic prefix, is given by $N_O = N_{CP} + Q$ in the discrete as well as by $T_O = T_{CP} + T_{SC}$ in the continuous domain. It is obvious that the CP leads to a reduction of the spectral efficiency introduced in the previous section by the factor of $Q/(Q + N_{CP})$. If the cyclic prefix is fixed and not adaptable to the current channel state there might be bad channel situations where the cyclic prefix interval is exceeded and ISI is unavoidable. Among others, one focus of this thesis is the analysis of these effects, in particular its impact on CoMP systems. A detailed analysis of the occurring interferences is given in chapter 3. In the following it is assumed that the CP is long enough so that *no* ISI occurs.

In multiple antenna systems the K transmitters explicitly use the same carrier frequencies

[13]See also appendix B.2.1.

[14]It should be noted that the cyclic extension is equal to the overlap and save approach for the fast convolution (see e.g. [Kam08]). A zero padding which is e.g. discussed in [MWG+02] would be equal to the overlap and add approach and also prevents ISI but has some implementation disadvantages.

so that the impinging waves of distinct sources are superimposed at the m-th receiver with:

$$y_o^m(t) = \sum_{k=1}^{K} \int_{\tau_C} h^{m,k}(\tau) x_o^k(nT_S - \tau)\mathrm{d}\tau + v(t) \tag{2.1.12}$$

where it is assumed that the channel impulse response is time invariant. The characteristics of the channel impulse response are discussed in more detail in appendix B.3.2. The term v again represents the additive noise distortion which is usually modeled as white Gaussian noise (AWGN). It should be noted that in Eq. (2.1.12) only the continuous time representation of the received signal is stated since in chapter 3 this expression is analyzed in more detail when the time and frequency asynchronisms are investigated. A corresponding discrete time model is provided in appendix C.1.

At the receiver the signal is transformed into frequency domain again by applying the Fourier transform to the subcarriers $q \in \mathcal{Q}$ so that the receive signal is obtained by:

$$Y_o^m(qB_{SC}) = \frac{1}{T_{SC}} \int_{T_{SC}} y_o^m(t)\; e^{\frac{-j2\pi qt}{T_{SC}}} \mathrm{d}t \tag{2.1.13}$$

Putting Eq. (2.1.12) in Eq. (2.1.13) leads to:

$$Y_o^m(qB_{SC}) = \frac{1}{T_{SC}} \int_{\mathcal{T}} \left(\sum_{k=1}^{K} \int_0^{\tau_C} h^{m,k}(\tau) \sum_{l \in \mathcal{Q}} X_{o,l}^k e^{\frac{j2\pi l(t-\tau)}{T_{SC}}} \mathrm{d}\tau + v^m(t) \right) e^{\frac{-j2\pi qt}{T_{SC}}} \mathrm{d}t \tag{2.1.14}$$

with $\mathcal{T} = \{t \in \mathbb{R} | oT_O \le t \le T_{SC} + oT_O\}$ as receiver integration interval. As long as the channel delay is shorter than the cyclic prefix length ($\tau_C < T_{CP}$) Eq. (2.1.14) can be rewritten as:

$$Y_o^m(qB_{SC}) = \sum_{k=1}^{K} \sum_{l \in \mathcal{Q}} X_{o,l}^k \frac{1}{T_{SC}} \int_{\mathcal{T}} e^{\frac{j2\pi(l-q)t}{T_{SC}}} \underbrace{\int_0^{\tau_C} h^{m,k}(\tau) e^{\frac{-j2\pi l\tau}{T_{SC}}} \mathrm{d}\tau}_{H^{m,k}(lB_{SC}) = H_l^{m,k}} \mathrm{d}t + V_o^m(qB_{SC}) \tag{2.1.15}$$

The frequency domain representation of the AWGN is given by:

$$V_{o,q}^m = V_o^m(qB_{SC}) = \frac{1}{T_{SC}} \int_{\mathcal{T}} v^m(t) e^{\frac{-j2\pi qt}{T_{SC}}} \mathrm{d}t \tag{2.1.16}$$

Due to the constant noise power spectral density N_0 it holds that $\sigma_v^2 = \sigma_V^2$. Furthermore, one can easily derive that[15]:

$$\int_{\mathcal{T}} e^{\frac{j2\pi(l-q)t}{T_{SC}}} \mathrm{d}t = e^{j\pi(l-q)}\; T_{SC} \;\mathrm{si}\left\{\pi(l-q)B_{SC}T_{SC}\right\} = \begin{cases} T_{SC} & (l-q) = 0 \\ 0 & \text{otherwise} \end{cases} \tag{2.1.17}$$

Obviously due to the utilization of a *cyclic* extension the linear convolution is turned into a

[15] Cf. Eq. (B.2.25) in appendix B.2.1.

circular convolution[16]. This result is one of the most important properties of OFDM systems since for frequency selective channels the ISI channel in time domain can be decomposed into parallel flat channels in frequency domain:

$$Y_{o,q}^{m} = \sum_{k=1}^{K} H_q^{m,k} X_{o,q}^{k} + V_{o,q}^{m} \;\Rightarrow\; \underline{Y}_{o,q} = \boldsymbol{H}_q \underline{X}_{o,q} + \underline{V}_{o,q} \tag{2.1.18}$$

with $\underline{X}_{o,q} \in \mathbb{C}^{K\times 1}$, $\underline{Y}_{o,q} \in \mathbb{C}^{M\times 1}$ as well as $\boldsymbol{H}_q \in \mathbb{C}^{M\times K}$. This equation is the well known simplified transmission equation where many known results of estimation[17] and information theory can be applied to. For instance, one can employ single tap frequency domain equalizers which are in particular very useful together with MIMO detection techniques which are briefly introduced in the following.

Receive Signal Combining: As it is known from classical estimation theory, when using multiple antennas the available observations need to be combined so that undesired signal components are suppressed while desired signal portions should be amplified. Assuming the same transmission model as stated in Eq. (2.1.18) onto each subcarrier q the matrix $\boldsymbol{H}_q$ must be inverted in order to reverse the coupling among the transmitters. Estimation theory provides a large number of solutions for estimating the input vector $\underline{X}_{o,q}$ by using the observations $\underline{Y}_{o,q}$. The optimum solution in terms of the mean squared error (MSE) always depends on whether the variables in Eq. (2.1.18) are handled as random or deterministic. Here it is assumed that the channel is fixed as well as that the noise symbols are distributed according to $\underline{\mathsf{V}}_{o,q} \propto \mathcal{N}_{\mathbb{C}}\left\{0, \boldsymbol{\Phi}_{\mathsf{VV}}\right\}$. Furthermore, the transmit symbols $\underline{\mathsf{X}}_{o,q}$ are taken uniformly at random from a discrete symbol alphabet $\mathcal{A}$ with covariance matrix $\boldsymbol{\Phi}_{\mathsf{XX},q} = \mathrm{E}_{\mathsf{X}}\left\{\left|\sqrt{\boldsymbol{P}_q}\underline{\mathsf{X}}_{o,q}\right|^2\right\}$. The diagonal matrix $\boldsymbol{P}_q \in \mathbb{C}^{K\times K}$ contains the individual transmit powers.

At this point only linear data estimation filters are introduced. The symbol detection which includes the demodulation and decoding of the transmitted information sequences is explained in detail in section 4.3. When using a linear filter matrix $\boldsymbol{G}_{o,q}$ which is multiplied to the available observation vector $\underline{\mathsf{Y}}_{o,q}$ the estimated transmit symbols are obtainable by:

$$\underline{\widehat{\mathsf{X}}}_{o,q} = \boldsymbol{G}_q \underline{\mathsf{Y}}_{o,q} = \boldsymbol{G}_q \left(\boldsymbol{H}_q \sqrt{\boldsymbol{P}_q} \underline{\mathsf{X}}_{o,q} + \underline{\mathsf{V}}_{o,q}\right) \tag{2.1.19}$$

In appendix B.1.2 the main results of linear estimation theory are introduced. The optimium solution w.r.t. the MSE for the previous problem is given by the linear least-mean-squares (LLMS) filter with:

$$\boldsymbol{G}_q = \left(\boldsymbol{\Phi}_{\mathsf{XX},q}^{-1} + \boldsymbol{H}_q^{\mathrm{H}} \boldsymbol{\Phi}_{\mathsf{VV}}^{-1} \boldsymbol{H}_q\right)^{-1} \boldsymbol{H}_q^{\mathrm{H}} \boldsymbol{\Phi}_{\mathsf{VV}}^{-1} \tag{2.1.20}$$

[16] See also appendix A.1.3 for a more detailed description of the circular convolution.
[17] In estimation theory these filters are also known as transform domain filters. See also [Say08].

The minimum costs can then be obtained by $\boldsymbol{\Phi}_{ee,q} = \left(\boldsymbol{\Phi}_{\mathsf{XX},q}^{-1} + \boldsymbol{H}_q^{\mathrm{H}}\boldsymbol{\Phi}_{\mathsf{VV}}^{-1}\boldsymbol{H}_q\right)^{-1}$. For uncorrelated transmit symbols of unit power with $\boldsymbol{\Phi}_{\mathsf{XX},q} = \boldsymbol{I}$ as well as AWGN with $\boldsymbol{\Phi}_{\mathsf{VV}} = \sigma_V^2\boldsymbol{I}$ Eq. (2.1.20) changes to the classical solution:

$$\boldsymbol{G}_q = \left(\boldsymbol{I}\sigma_V^2 + \boldsymbol{H}_q^{\mathrm{H}}\boldsymbol{H}_q\right)^{-1}\boldsymbol{H}_q^{\mathrm{H}} \tag{2.1.21}$$

which converges to the well known least-squares (LS) solution for low noise power values $\sigma_V^2 \approx 0$. The post-equalization SINR for the k-th user at the combiner output, which is often used as performance measure, can be stated as:

$$\Gamma_q^k = \frac{p_q^k \left(\underline{\widetilde{G}}_q^k\right)^{\mathrm{H}} \underline{H}_q^k \left(\underline{H}_q^k\right)^{\mathrm{H}} \underline{\widetilde{G}}_q^k}{\sum_{i=1,i\neq k}^{K} p_q^i \left(\underline{\widetilde{G}}_q^k\right)^{\mathrm{H}} \underline{H}_q^i \left(\underline{H}_q^i\right)^{\mathrm{H}} \underline{\widetilde{G}}_q^k + \left(\underline{\widetilde{G}}_q^k\right)^{\mathrm{H}} \boldsymbol{\Phi}_{\mathsf{VV}}\underline{\widetilde{G}}_q^k} \tag{2.1.22}$$

with $\underline{\widetilde{G}}_q^k$ denoting the k-th column vector of the matrix $\widetilde{\boldsymbol{G}}_q = \boldsymbol{G}_q^{\mathrm{H}}$ and $p_q^k = \boldsymbol{\Phi}_{\mathsf{XX},q}[k,k]$. When assuming the LLMS filter according to Eq. (2.1.21) the SINR and the MSE are coupled via $\Gamma_q^k = (1 - \boldsymbol{\Phi}_{ee,q}[k,k])/\boldsymbol{\Phi}_{ee,q}[k,k]$.

Spectral Efficiency: The achievable capacity for general transmission models was already discussed in section 2.1.1. Here, the discussion is continued for the MIMO OFDMA model which is the basis throughout this work. When using a linear combiner as stated in Eq. (2.1.20) the coupling among the transmit symbols is reversed so that the maximum spectral efficiency depends on the SINR at the combiner output and can be approximated by Eq. (2.1.1). Assuming a transmission on $N_{SC} = |\mathcal{Q}|$ subcarriers the achievable spectral efficiency can be stated as:

$$\frac{\widetilde{C}}{\mathrm{bit/s/Hz}} = \sum_{q\in\mathcal{Q}}\sum_{k=1}^{K} \mathrm{ld}\left(1 + \Gamma_q^k\right)/(Q + N_{CP}) \tag{2.1.23}$$

where the additional overhead caused by the cyclic prefix and unused subcarriers in OFDM is already considered. As it was introduced in Eq. (2.1.2) the maximum sum capacity for those transmission systems is given by[18]:

$$\frac{\widetilde{C}}{\mathrm{bit/s/Hz}} = \sum_{q\in\mathcal{Q}}\sum_{i=1}^{\kappa_q} \mathrm{ld}\left\{1 + \lambda_{i,q}\frac{p_q^k}{\sigma_V^2}\right\}/(Q + N_{CP}) \tag{2.1.24}$$

with $\kappa_q = \mathrm{rank}\left\{\boldsymbol{H}_q\boldsymbol{H}_q^{\mathrm{H}}\right\}$ and $\lambda_{i,q}$ as the non-zero eigenvalues of $\boldsymbol{H}_q\boldsymbol{H}_q^{\mathrm{H}}$. As discussed in [SB04], in order to balance the post-equalization SINR at each subcarrier a power allocation p_q^k in spatial domain (indicated by index k) can be applied. Furthermore, as widely known the optimal power allocation across the subcarriers (indicated by index q) can be achieved by using

[18]See also [Tel99] or appendix B.2.3.

the waterfilling theorem with a sum power constraint given by Parseval's theorem[19]. However, for the sake of simplicity it is often assumed that all users transmit with full power which is equally distributed among all subcarriers so that $p_q^k = P_{max}/N_{SC}$ with P_{max} as maximum transmit power per user at the antenna output.

As mentioned above, in Eq. (2.1.24) the spectral efficiency is already scaled in order to take the overhead of the unused subcarriers as well as the cyclic prefix into account. A question that often arises is how much overhead should be spent to obtain the maximum spectral efficiency? As the spectral efficiency directly depends on the post equalization SINR a loss of spectral efficiency is equal to an SINR loss. Assume a real scaler $\beta_C \leq 1$ that represents a required overhead, e.g. for additional pilot subcarriers or cyclic prefix samples, as well as that for $\beta_C = 1$ the *average* SINR $\overline{\Gamma}$ is achieved. For $\overline{\Gamma} \gg 1$ the average SINR gain a_C which is obtained due to the signaling overhead must be approximately larger than[20]:

$$a_C > \overline{\Gamma}^{1/\beta_C - 1} \tag{2.1.25}$$

in order to increase the spectral efficiency. For instance, when using the long instead of the short cyclic prefix in a 3GPP/LTE system a loss in spectral efficiency of $\beta_C = 6/7$ must be considered (Cf. [3GP11d]). Assume that an SINR of 20 dB is achieved when using the short cyclic prefix. Then, at least an SINR gain of ≈ 3 dB is needed before it is more efficient to switch to the long cyclic prefix mode.

2.2. Cooperative Cellular Wireless Networks

As already mentioned in the previous section, CoMP systems are similar to SDMA systems. In conventional wireless communication systems the SDMA principle is already used as well but with the restriction that the users which transmit on the same resource need to be decoupled by the pathloss attenuation so that the channel is quasi orthogonalized and a single base station only serves users on orthogonal resources. Therefore, joint signal processing is used to extend the idea of SDMA also to the cell edge users where multi-user interference limits the system performance. This section is intended to discuss implementation issues of MIMO techniques on the cellular level. This concerns in particular effects of the propagation channel which are distance dependent such as pathloss and propagation delays. Therefore, in the following the impact of the pathloss on the link separation as well as the occurring timing delays in multi-point to multi-point systems are investigated which have a direct impact on the OFDM parameter design.

[19]See also appendix B.2.1.
[20]Solve $\mathrm{ld}\left(\overline{\Gamma} \times a_C\right) \beta_C - \mathrm{ld}\left(\overline{\Gamma}\right) > 0$

2.2.1. Base Station and User Clustering

The simplest assumption is that all transmit or receive data is always available to all base stations. This is the case when considering a centralized joint signal processing within one core unit and geographically separated remote antenna units connected via high speed fiber links[21]. The same holds for intra-site cooperation where the signal processing units are located at the same position in the network and no additional backhaul is required to exchange the information needed for cooperation. For simplicity, throughout this work it is always assumed that the data is available at each base station which actually implies an infinite backhaul for decentralized inter-site cooperation. In real networks the impact of the backhaul would also include:

- Quantization effects due to limited backhaul rate.
- Additional signal delays that depend on the backhaul network structure.

It should be noted that the impact of a constrained backhaul on the system performance is not considered throughout this thesis. The reader is referred to [Mar10] for more informations about this implementation issue.

When clustering N_{BS} base stations or cells that should apply a joint signal processing for a cluster of N_{UT} users the most important metric is the achievable SNR on each link between one user and one base station. Therefore, in the following the underlying pathloss and power control model is briefly introduced. Thereafter, the link separation is discussed which represents the decision metric for the base station and user clustering throughout this work.

Pathloss Model: The characteristics of the wireless channel links between the base stations and the users in the network are mainly of stochastic nature. The dominant effects are described in detail in appendix B.3. Basically, the average attenuation of the electro-magnetic field between the transmit and receive antenna is given by the distance dependent pathloss which is superimposed by various random effects such as large and small-scale fading. With a given link budget the random[22] receive power level P_R at each location in the network can be stated as:

$$\frac{\mathsf{P}_R(d)}{[\text{dBm}]} = \frac{P_T}{[\text{dBm}]} + \frac{A_G}{\text{dB}} - \frac{\mathsf{a}(d)}{[\text{dB}]} - \frac{a_{margin}}{[\text{dB}]} = \frac{P_T}{[\text{dBm}]} - \frac{\tilde{\mathsf{a}}(d)}{[\text{dB}]} - \frac{a_{margin}}{[\text{dB}]} \tag{2.2.1}$$

where P_T is the transmit power and A_G the sum of transmit and receive antenna gains. The random distance dependent pathloss is given by $\mathsf{a}(d)$ and a_{margin} contains a prediction margin. When using directive antenna patterns the co-channel interference can be reduced compared to an uniform signal radiation in each direction given by an omni-directional antenna pattern. As mentioned above, all variables are discussed in detail in appendix B.3.1.

[21] Radio-over-fiber links are e.g. introduced in [HLH+10].

[22] Random w.r.t. the large-scale fading but average according the small-scale fading.

Parameter	Value
Carrier freq.	$f_C = 800$ MHz
Signal / subcarrier bandwidth	$B_S = 1.92$ MHz / $B_{SC} = 15$ kHz
DFT size / OFDM symbol period	$Q = 128 \triangleq T_{SC} = 66.7\ \mu$s
Used subcarrier / data bandwidth	$N_{SC} = 120 \triangleq B_{DSC} = 1.8$ MHz (around dc)
Cyclic prefix length	$\Lambda = 9 / 32 \triangleq T_{CP} = 4.7 / 16.7\ \mu$s (Short/Long)
Cooperation cluster size	$N_{BS} = 2 / N_{UT} = 2$
BS / UT antenna number	$N_{BS,ant} = 1 / N_{UT,ant} = 1$
Maximum transmit power	$P_{max} = 23$ dBm
Noise power per subcarrier	$\sigma_v^2 = -111$ dBm
Large scale fading scenario	Rural Macro PL, random LOS/NLOS and shad.
Small scale fading scenario	Rural Macro PDP, no spatial correlation
Default inter-site distance	ISD = 5000 m
Default target SNR	$\Gamma_{target} = 20$ dB

Table 2.1.: Default simulation parameters

For an exemplary pathloss scenario in Fig. 2.3 the maximum obtainable receive power for an omni as well as directive antenna pattern is shown. The used pathloss specifications are also defined in appendix B.3.1 and represent a rural environment. The basic parameters for the numerical computer simulations are stated in Tab. 2.1. To avoid border effects in total 27 cells are generated. The cell area of interest consists of three inner cells where the base stations are located in the middle of a cell for omni-directional signal radiation as well as at the cell corner for a sectorized antenna pattern. The occurrence of a line-of-sight (LOS) instead of a non-line-of-sight (NLOS) path is chosen randomly. Therefore, Fig. 2.3 represents only a snapshot of one possible realization of the occurring pathloss attenuations which leads to an inhomogenous distribution of the receive powers within the depicted cell area. As one can observe, in such scenarios also at the cell edge there might be situations where a strong LOS path occurs so that e.g. a user who is actually far apart from a base station becomes a dominant interferer. Thus, a main conclusion at this point is that when considering stochastic pathloss models the geographic distance between the base stations and the terminals is not deterministically coupled to the achievable receive power levels. As will be seen later, this aspect becomes important when considering the occurring timing delays which are also also distance dependent.

Power Control: In wireless networks with multiple users and base stations the signal power at one base station in the uplink consists of many different contributions from different users. In order to reduce the multi-user interference as well as to save energy, the users usually adjusts

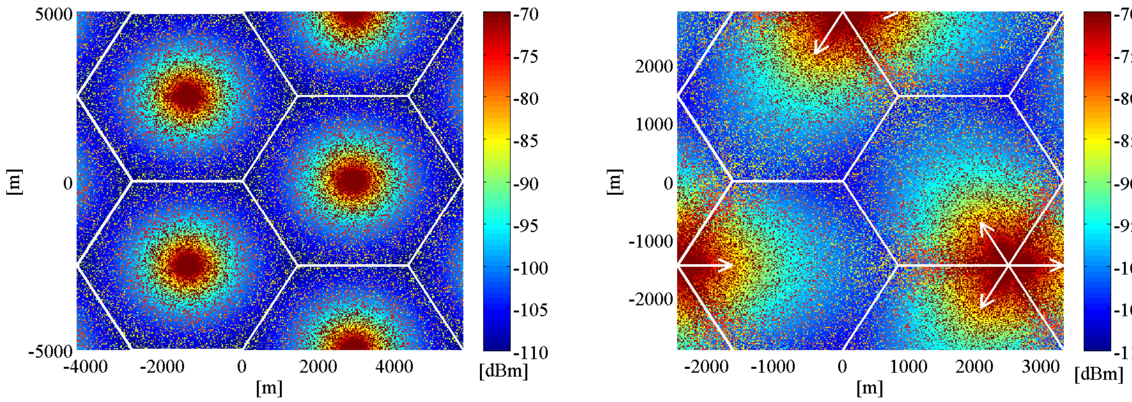

Figure 2.3.: Exemplary maximum receive power levels for a hexagonal cell setup with an omni-directional (left) and sectorized (right) base station antenna pattern (Simulation parameter as defined in Tab. 2.1, only random LOS/NLOS).

its effective radiated power to achieve an SNR required for a reliable signal transmission. The link SNR $\gamma^{m,k}$ at the m-th receive antenna input for user k is given by:

$$\frac{\gamma^{m,k}_{link}}{[\text{dB}]} = \frac{\mathsf{P}^{m,k}_R(d)}{[\text{dBm}]} - \frac{P^m_V}{[\text{dBm}]} = \frac{P^k_T}{[\text{dBm}]} - \frac{\tilde{\mathsf{a}}^{m,k}(d)}{[\text{dB}]} - \frac{P^m_V}{[\text{dBm}]} \tag{2.2.2}$$

with P_V as noise power level that depends on the signal bandwidth and the constant power spectral density N_0 of the noise. Due to the exponential relation of the distance and the pathloss particularly at positions close to a base station very high receive power levels would be observable. However, the maximum observable SNR at the receiver is limited by the ADC resolution[23]. As already discussed in section 2.1.1, the optimal power allocation is given by the water-filling theorem but this would only make sense if the transmitters as well as the receivers are able to cooperate as it is the case in single link MIMO systems. Furthermore this strategy is optimal for the sum capacity but does not consider the user fairness. Otherwise the transmit power needs to be controlled to achieve individual target SNRs which is a more user centric measure.

In the uplink the power adjustment is done by the terminals separately. Therefore, the base stations estimate the instantaneous receive power level $P^{m,k}_R$ between user k and base station m and calculate the terminal transmit powers w.r.t. a target link SNR that should be achieved at one certain base station. These estimates are then fed back to the terminals and used to adapt the transmit power. When choosing the base station with the maximum receive power level of user k the transmit power for this user is calculated by:

$$\frac{P^k_T}{[\text{dBm}]} = \min\left\{\frac{P^m_V}{[\text{dBm}]} + \min_m\left\{\frac{\tilde{a}^{m,k}(d)}{[\text{dB}]}\right\} + \frac{\gamma^{m,k}_{target}}{[\text{dB}]}, \frac{P_{max}}{[\text{dBm}]}\right\} \tag{2.2.3}$$

which represents the simplest case of an closed loop power control. It should be noted that

[23] See e.g. [Löh06] for a detailed ADC analysis.

the maximum transmit power is again constrained to P_{max}. Throughout this work only this power control strategy is assumed. For more advanced techniques of iterative power control the reader is referred to [Yat95] or [Zan92].

Link Separation: As mentioned before, the transmit power of the users is limited. Thus, in terms of the receive power levels measurable at the base station antennas it might become difficult to achieve the target SNR levels on all links. In order to exploit the best trade-off between joint and single base station signal processing, there are requirements in terms of the minimum receive power level. A convenient metric to assess the decoupling of two links is the separation factor (SF) that defines the ratio between the maximum and minimum receive power of one k-th terminal observed at all N_{BS} base stations in the cooperation cluster[24]:

$$\Delta a = \frac{\max\limits_{m} \left\{ P_R^{m,k}(d) \right\}}{\min\limits_{m} \left\{ P_R^{m,k}(d) \right\}} = \left(\frac{d_{max}}{d_{min}} \right)^{\eta} \tag{2.2.4}$$

where it is assumed that the receive power level mainly depends on the distance between the base stations and the user terminal as well as the shadowing fading. The second term only holds for omni-directional signal radiation without sectorization as well as a deterministic pathloss model. This expression should illustrate the simplest case where the link separation only depends on the geographic distances as well as the pathloss exponent η.

It should be noted that the geometry factor, as e.g. described in [MF11], includes also the total interference power contribution from all non-desired links while the link separation introduced here only compares the maximum and the minimum receive power contribution. As the receive signals from all links within a cooperation cluster should be exploited in a joint signal processing at this point the link separation metric is useful to precisely bound the cooperation regions. Clearly, these regions mainly depend on the cooperation cluster size. When using the link separation factor it is possible to define a certain cell edge region in which the maximum link separation is below a defined threshold $\Delta a \leq \alpha$. Furthermore, it turned out that cooperation among base stations only makes sense in a defined cooperation range α which expresses the trade-off between benefits of cooperation and losses due to the overhead of extended signal processing. Moreover, if more than one user is served by the base station cluster it should be ensured that all terminals in the cluster have their strongest links to the *same* base stations.

On the left-hand side of Fig. 2.4 the distribution of the occurring link separation values are shown for different values of the cooperation range α and a fixed value of the pathloss exponent. Again the pathloss model as stated in Tab. 2.1 is used for the computer simulations. For obtaining the simulation results the users are uniformly distributed within the cell edge region defined by α. As one can observe, the CDF does not increase linearly. Even for high

[24] It should be noted that this metric represents a user specific clustering.

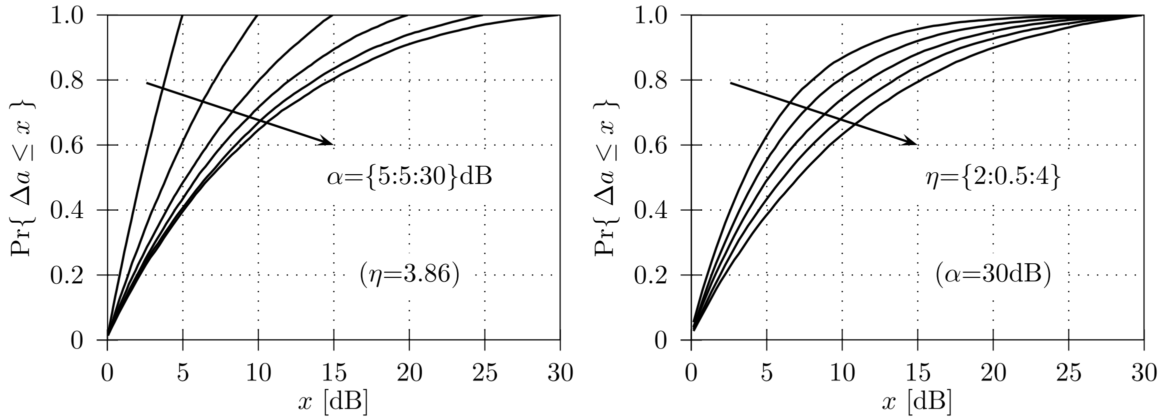

Figure 2.4.: Distribution of occurring link separation values for different values of cooperation ranges α (left) and different pathloss exponents η (right) (Cell setup as defined in Tab. 2.1, only random shadow fading, NLOS, omni-directional antenna pattern).

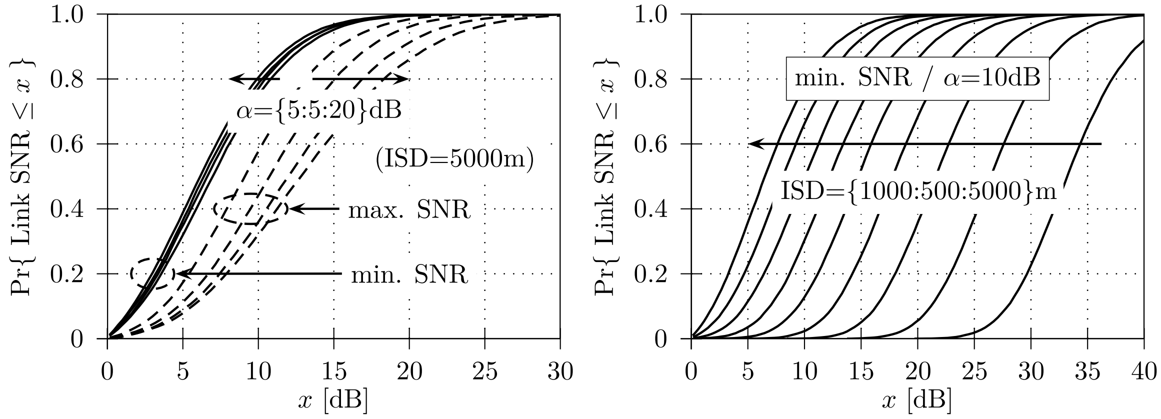

Figure 2.5.: Distribution of occurring link SNR values for different values of cooperation ranges α (left) and different ISDs (right) (Cell setup as defined in Tab. 2.1, only random shadow fading, NLOS, omni-directional antenna pattern).

cooperation ranges the probability decreases that such extreme scenarios occur. The reason for that lies in the cell geometry since the signal radiation is omni-directional while the cells have a hexagonal structure. On the right-hand side of Fig. 2.4 the impact of the pathloss exponent is shown. As expected, the lower the pathloss exponent is the more balanced the receive power levels become. On the left-hand side of Fig. 2.5 for an ISD of 5000 m the distributions of the minimum and maximum occurring link SNRs for different cooperation ranges are depicted. As one can see, by increasing the cooperation range particularly the probability of larger maximum link SNRs increases. On the right-hand side of Fig. 2.5 the distribution of the minimum link SNRs is shown for a fixed cooperation range of 10 dB and different inter-site distances. It should be noted that for this evaluation no power control is applied and users always transmit with full power. The results illustrate that, of course, particularly for large inter-site distances the SNR levels observable at non-serving base stations may not fulfill a given quality of service requirement.

2.2.2. Network Synchronization

Since the main focus of this thesis is the investigation of the impact of asynchronisms on the CoMP performance the two important aspects of time as well as frequency synchronization are discussed here. As it is the case for the power alignment, also in terms of frame timing and carrier frequency the base station network serves as a reference for all terminals. Thus, the synchronization must be ensured twofold. On the one hand, the network itself must operate in total synchrony which is only an ideal assumption and on the other hand synchronization procedures are needed in order to align the terminals to the network reference. The main synchronization problems which have to be overcome are:

- Inter-BS frequency synchronization for phase coherent joint signal processing.
- Inter-BS time synchronization in order to ensure a consistent frame timing among all base stations.
- Timing synchronization of the terminal in the downlink in order to compensate the downlink propagation delay.
- Frequency synchronization of the terminals in the downlink in order to avoid a spectral leakage as described in chapter 3.
- Pre-compensation of the uplink propagation delays by applying a timing advance value which is estimated by the base stations and fed back to the terminal via the downlink as it is also the case for the power control.

The synchronization requirements for 3GPP/LTE networks are described in detail in [3GP11f]. Particularly the short term frequency stability for the base stations is specified with $0.5 \cdot 10^{-7}$ over a period of 1 ms (Cf. [3GP11a]) as well as for user terminals with 10^{-7} over a period of 0.5 ms (Cf. [3GP11g]). As an example, for a carrier frequency of 2.6 GHz this would require a maximum frequency deviation of $\approx$ 130 Hz for the base stations and $\approx$ 260 Hz for the user terminals, respectively.

Imperfect Base Station Synchronization: As mentioned above, the assumption that the base station network operates in full synchrony is an idealized model. A comprehensive overview about practical challenges connected to the synchronization of CoMP networks is e.g. given in [JWS+08] as well as in [MF11]. Single frequency networks are well known from other broadcast services such as television. Probably the best known single frequency networks are the global navigation satellite systems (GNSS) such as GPS[25]. Single frequency networks always aim at providing a constant frame timing as well as frequency stability. Intuitively, it is evident that a high frequency stability also implies a good timing accuracy. The best accuracy would be achievable by using only high precision oscillators for the impulse generation. In Tab. 2.2 the achievable performance values of different oscillator types are stated. As one can see, the more

[25] GPS $\triangleq$ Global Positioning System

Parameter	**TCXO**	**MCXO**	**OCXO**	**Rubidium**
Short Term Stability (Δf/f, t=1 s)	$\approx 1x10^{-9}$	$\approx 3x10^{-10}$	$\approx 1x10^{-12}$	$\approx 3x10^{-12}$
Long Term Aging (Δf/f, t=1 year)	$\approx 5x10^{-7}$	$\approx 2x10^{-8}$	$\approx 5x10^{-9}$	$\approx 2x10^{-10}$
Price in $	$\approx$ 100	$\approx$ 1000	$\approx$ 2000	$\approx$ 8000

Table 2.2.: Oscillator comparison (values taken from [VB99])

precise the devices are the more expensive they become which makes it unprofitable to equip all base stations with such hardware.

Therefore, one solution is to use the GNSS signals for clock synchronization. For instance, the GPS satellites contain Rubidium as well as Cesium atomic normals which deliver high frequency precision up to 10^{-13}. In general, satellite systems for navigation purposes are optimized to have a very good long term stability. A conventional GPS receiver provides the 3D coordinates of the receiver location as well as a stable one pulse per second which can be used for frame timing synchronization in the base stations. If only the stable clock signal is needed the receiver must be connected to at least one GPS satellite which cannot be ensured in all regions due to the low receive power level of the GPS signals, particularly in indoor scenarios. Therefore, a GPS receiver itself must be equipped with a quartz oscillator with good short term stability to overcome a GPS outage. For that reason GNSS based synchronization remains an expensive solution for practical deployments.

Alternatives to GNSS synchronization are network protocols such as the network time protocol as well as the precision time protocol which is also referred to as IEEE 1588 protocol according to the corresponding standard. Those protocols work in a hierarchical manner with master nodes which are highly synchronized and slave nodes which derive their synchrony in time by exchanging time stamp messages with the master nodes. Clearly, as it holds for all network protocols the performance of these techniques strongly depends on the network architecture but thus they also provide a high flexibility. A performance comparison of all introduced synchronization methods is given in Tab. 2.3. The most promising solution for practical deployments in wireless networks in terms of a sufficient accuracy as well as costs is probably the precision time protocol[26].

As mentioned above, in centralized CoMP networks the data signals must be conveyed to the remote antenna units. In those systems the signal delays caused by different cable lengths must be taken into account. A rule of thumb is that the effective length of a connection between the core units as well as the remote antenna units are approximately five times larger than the line-of-sight distances. If for example the radio over fiber technology is supposed to be used, as

[26] Cf. [MF11]

Parameter	Time	Freq.	Costs
GNSS	≈ 100 ns	$\approx \pm 10^{-12}$	high (Cf. Tab. 2.2)
Network Time Protocol	$\approx$ ms	$\approx \pm 10^{-7}$	low
Precision Time Protocol	$\approx 1\ \mu$s	$\approx \pm 10^{-8}$	low

Table 2.3.: Performance comparison of network synchronization techniques (values taken from [MF11, Ch. 8])

introduced in [HLH+10], the reduced signal speed within the fibers must be considered which is characterized by the refractive index as the loss w.r.t. the speed of light. The values of the refractive index typically lie in the region of 1.45. If these delays are relatively constant over time it is possible to use variable time-delay modules which are able to compensate those additional delays and ensure that the signals at the remote antenna unit antennas have the same timing behavior.

Terminal Synchronization: The signals between the user terminals and the base stations are propagated through the air and arrive at the receiver with a delay caused by the limited speed of light. With $c_{light} \approx 3 \cdot 10^8$ m/s an illustrative expression is that the wave travels 300 m/μs which is in the order of symbol intervals of common wideband communication systems ($T_S < 1\ \mu$s) and could be resolved after sampling. If d_{BS-UT} denotes the path distance between one user terminal and one base station, the time of arrival can simply be calculated by [27]:

$$t_0 + \tau_d = t_0 + d_{BS-UT}/c_{light} \tag{2.2.5}$$

with t_0 as frame timing reference point used within the transmitter. Since the base stations cannot pre-compensate any timing delay in the downlink broadcast channel, the user terminals must compensate these signal delays by using appropriate algorithms. Furthermore, in the uplink multiple access channel the base station cannot post-compensate time asynchronisms among users. Therefore, they estimate the timings from all users and feed back these estimates so that the terminals can pre-compensate the supposed timing delays in advance. A similar procedure is applied for frequency synchronization where the local oscillator in the terminal is adapted to the estimated offset w.r.t. the base station network. Particularly for OFDM systems there are numerous algorithms for time and frequency synchronization. A good overview about state of the art algorithms is given in [vdBBB+99] or [SFFM99] for OFDM in general as well as in [MKP07] for the application to cellular systems. The extension to multiple antenna systems is straight forward and can e.g. be found in [HB08]. A case study of the application of synchronization algorithms for a 3GPP/LTE downlink synchronization as well as cell search is e.g. presented in [MGEJ+09]. Some of those algorithms are also discussed in

[27] Signal delays caused by the radio channel are also discussed in appendix B.3.2 in more detail.

more detail in chapter 5 where the focus is on parameter estimation in general.

An interesting metric is the minimum achievable estimation error of the synchronization algorithms in order to get a rough guide about the average timing and frequency error. The minimum variance is given by the Cramer-Rao lower bound (CRLB) as introduced in appendix B.1.1 which can be achieved with a Maximum-Likelihood estimator at least for a large number of observations. For a simple single tone frequency estimator the CRLB is derived in appendix B.1.1. Normalized to the subcarrier bandwidth the CRLB is obtainable by:

$$\mathrm{CRLB} = \frac{1}{\mathrm{SNR}} \frac{6}{(2\pi T_S)^2 N(N^2-1)} \frac{1}{B_{SC}^2} \tag{2.2.6}$$

Here, N denotes the number of observations usable for estimation purposes. For the timing estimation the minimum error variance is similar as the timing shift in time domain can be treated as increasing phase in frequency domain. Thus, the bound in Eq. (2.2.6) roughly holds for both estimators, but in different domains. Assume $N = 512$ available observations, a sampling interval of $T_S = 1/30.72$ MHz as well as an SNR of 10 dB. This would lead to an average deviation of the frequency shift of $\approx \pm 0.02 \times B_{SC}$ as well as to an average timing shift of $\approx \pm 0.02 \times T_S$. When testing other SNR values or number of observations one can conclude that in theory a quite reliable estimation of the integer symbol timing offset is possible while the estimation of the frequency mismatch will lead to errors that will affect the overall system performance as will be seen later on.

However, it should be noted that the CLRB represents a *lower bound*. Usually in OFDM systems with a cyclic prefix the optimal timing point for starting the discrete Fourier transform is usually specified to cover small synchronization inaccuracies. If the standard deviation for an estimator is e.g. set to $\approx \pm 0.05 \times T_{CP}$ the optimum timing point needs to determined with $t_{DFT,start} = t_0 \pm 0.05 \times T_{CP}$. Thus, in total a length of $\tau_{est} = 2 \cdot 0.05 \times T_{CP}$ must be reserved for estimator failures for avoiding a misplaced DFT window which leads to inter-symbol as well as inter-carrier interference as investigated later in chapter 3.

Timing Delays in CoMP Networks: So far only single links are discussed. In cooperative networks multiple links must be considered which are detectable by one receiver. If one assumes that the locations of the base stations can be far apart, particularly in deployments with large inter-site distances[28], e.g. in rural areas, it is necessary to take also the time differences of arrival at the receiver into account. As mentioned earlier, TDOAs are unavoidable in cooperative networks since for example in the uplink of a cellular system the terminals can align their timings only with respect to one base station which is usually the serving one. To the other base stations the user terminals are unsynchronized. As we are explicitly interested in exploiting the signal propagation between base stations and terminals across multiple cells the TDOAs must be treated as symbol timing offsets at base stations where the users are *not* aligned in

[28]In 3GPP/LTE up to an ISD of 5 km the maximum specified performance must be feasible (Cf. [STB09]).

time. The maximum TDOA at the m-th receiver branch is given as the difference between the minimum and maximum time of arrival (ToA):

$$\Delta\tau_{d,max}^{m} = \tau_{d,max}^{m} - \tau_{d,min}^{m} = \left(d_{max}^{m} - d_{min}^{m}\right)/c_{light} \tag{2.2.7}$$

with d_{max} and d_{min} as the maximum and minimum distance between the receiver and more than one transmitter.

As discussed previously, in order to avoid inter-symbol interference in OFDM systems the cyclic prefix needs to be designed to cover various effects such as:

- Asynchronisms within the base station network, e.g. $\tau_{BS} \approx 1\ \mu$s as maximum delay among two base stations within a cooperation cluster using the precision time protocol.
- Estimation errors due to synchronization algorithms, e.g. $\tau_{est} = 0.1 \times T_{CP} \approx 0.5\ \mu$s assuming a cyclic prefix length as specified by 3GPP/LTE with $T_{CP,short} = 4.7\ \mu$s.
- Small scale time differences of arrival which are referred to as channel delay spread caused by the multi-path propagation between one transmitter and one receiver as e.g. described in appendix B.3.2. In rural areas these multi-path delays are in the region of $\tau_C \approx 0.5\ \mu$s but also can achieve up to $\tau_C \approx 18\ \mu$s in hilly terrains[29].

Under these assumptions a total timing margin of $\approx 2\ \mu$s must be considered[30] so that the maximum path difference among two transmitters is restricted to:

$$\Delta\tau_{d,max}^{m} \leq T_{CP,short} - \tau_{C,rural} - \tau_{BS} - \tau_{est} \approx 2.7\ \mu\text{s} \;\Rightarrow\; \Delta d_{max} \approx 810\ \text{m} \tag{2.2.8}$$

Clearly this is only a conservative estimate and in real applications the maximum allowed TDOA is probably smaller. In 3GPP/LTE there is also a long cyclic prefix available with a length of $T_{CP,short} = 16.7\ \mu$s which allows larger TDOAs. But one has to keep in mind that this results in a loss of spectral efficiency of 1/7 since one OFDM symbol out of 7 within a LTE time slot is omitted. Therefore, one main question in this work is whether the loss of spectral efficiency due to the occurring inter-symbol interference is worse than the loss due to the usage of a cyclic prefix that covers all possible TDOAs? The idea behind this question is that the already introduced pathloss also leads to an attenuation of the asynchronous interference terms so that they are less severe than one might expect. This effect is discussed in detail in section 3.2. In the following the maximum possible cooperation radius is investigated which is limited by the cyclic prefix as well as pathloss conditions.

Maximum Allowed Cooperation Radius in CoMP: In Fig. 2.6 a simple 2×2 symmetric user positioning model is depicted where two users move from the cell edge ($r_C = 0$ m/ $\Delta\tau_d =$

[29] Cf. [3GP11b]

[30] It should be noted that this "time" budget is only usable as a simple illustration for one specific scenario. All stated parameters actually must be treated as random and not as fixed values.

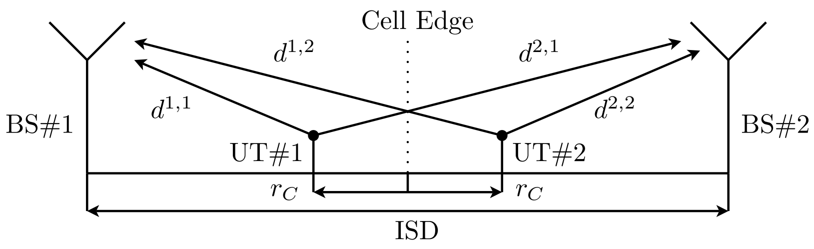

Figure 2.6.: Symmetric user positioning scenario with two users and two base stations

0 μs) to their serving base stations. Thus, the distances between the users and base stations can explicitly be stated with $d^{1,1} = d^{2,2} \approx \text{ISD} - r_C$ and $d^{1,2} = d^{2,1} \approx \text{ISD} + r_C$. Each base station applies a time and frequency synchronization with resprect to the direct user so that at one base station always one aligned and one unaligned user can be observed. If the signal power of the primary user at the receive antenna is adjusted to have unit average power the unaligned user is attenuated according to the link separation value Δa. As one can see, the users are located within a cooperation radius r_C around the cell edge so that the maximum link separation according to Eq. (2.2.4) is given by[31]:

$$\Delta a_{max} = \alpha = \left(\frac{d_{max}}{d_{min}}\right)^{\eta} = \left(\frac{\text{ISD}/2 + r_{C,SF}}{\text{ISD}/2 - r_{C,SF}}\right)^{\eta} \tag{2.2.9}$$

with $r_{C,SF}$ as cooperation radius for which the limit α is achieved. The maximum cooperation radius in terms of the TDOA can be obtained by using the rough bound of Eq. (2.2.8) with $r_{C,TDOA} \approx \Delta d_{max}/2$. As a result the maximum inter-site distance can be obtained by:

$$r_{C,TDOA} = \Delta\tau^{m}_{d,max} \times c_{light} \leq \frac{\text{ISD}\left(\alpha^{1/\eta} - 1\right)}{2\left(\alpha^{1/\eta} + 1\right)} \;\Rightarrow\; \text{ISD} \leq \frac{\Delta d_{max}\left(\alpha^{1/\eta} + 1\right)}{\left(\alpha^{1/\eta} - 1\right)} \tag{2.2.10}$$

If one assumes a pathloss exponent with $\eta = 3.86$ as stated in Tab. B.2 for the 3GPP/LTE rural macro NLOS case as well as a cooperation range of α =20 dB, the maximum distance among the base stations would be limited to ISD $\approx$ 1500 m. In the case of larger inter-site distances the TDOAs would inherently affect the transmission performance and either the cooperation radius must be reduced further or one has to cope with the asynchronisms. For instance, an ISD of 5000 m would lead to a theoretical cooperation range of $r_{C,SF} \approx 1340$ m which is more than three times larger than the maximum allowed radius $\Delta d_{max}/2 \approx 405$ m limited by the TDOA. On the left-hand side of Fig. 2.7 the theoretical extension of the cyclic prefix according to Eq. (2.2.10) is shown for which the entire cooperation range can be exploited. Based on the underlying timing error model of Eq. (2.2.8) different inter-site distances as well as cooperation ranges are investigated. For example, when using the short cyclic prefix in LTE the maximum allowed ISD for which the entire cooperation range of $\alpha = 10$ dB can be exploited is limited to $\approx$ 2.7 km. For an ISD of 5 km an cooperation range of only 5 dB would be possible without

[31] Here, again for simplicity a omni-directional antenna pattern is assumed.

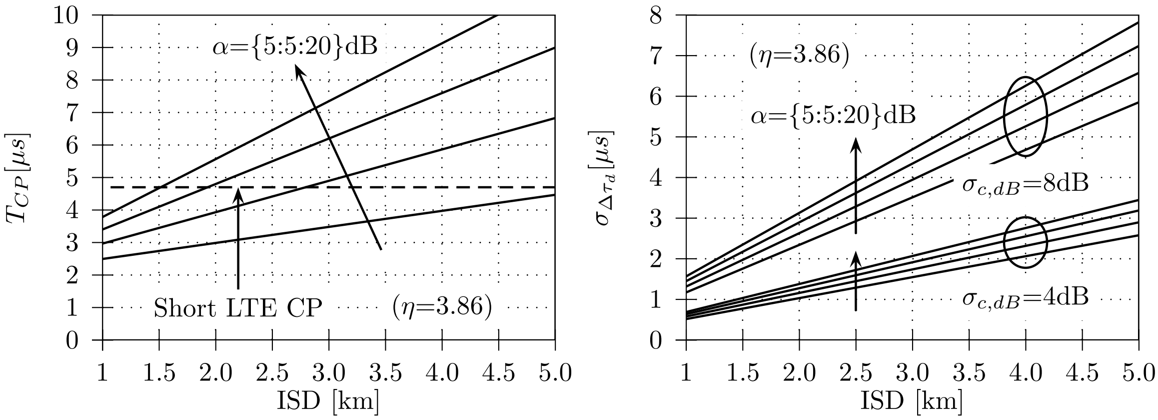

Figure 2.7.: Required extension of the cyclic prefix length (left) and average timing error for different ISD and cooperation ranges (right)

violating the CP limit.

As mentioned above, the pathloss values must be treated as random so that also users might be in the cooperation range which are farther away from the cell border than the specified cooperation radius $r_{C,SF}$ and thus cause higher TDOAs. The random nature of the pathloss is mainly characterized by the shadow fading. If $\sigma_{c,dB}$ denotes the standard deviation of the shadow fading in the log domain the average timing error can be approximated with:

$$\sigma_{\Delta\tau_d} = (\mathrm{ISD}/2 + r_{C,SF}) \left(10^{0.1\sigma_{c,dB}/\eta} - 1\right) / c_{light} \qquad (2.2.11)$$

The previous expression represents the average timing difference between the user position at $d^{1,2} = d^{2,1} = \mathrm{ISD}/2 + r_{C,SF}$ as well as the distance from this location which corresponds to a pathloss difference of $\sigma_{c,dB}$. Particularly for large inter-site distances the timing error will increase. On the right-hand side of Fig. 2.7 the average timing error is shown for different inter-site distances, cooperation ranges as well as standard deviations of the shadow fading. As expected, with higher ISDs the timing error becomes larger. When taking the previous example and assuming a cooperation range of 10 dB, an ISD of 2.7 km as well as a shadow fading of $\sigma_{c,dB} = 8$ dB an average timing error of ≈ 3.5 μs can be expected.

Similar values can also be observed in Fig. 2.8. There, the distribution of TDOAs that occur for different inter-site distances as well as cooperation ranges are depicted for a random user positioning with and without shadowing for a hexagonal cell setup as depicted in Fig. 2.3. On the left-hand side the cooperation range is fixed to 10 dB and the ISD is varied. As one can see, without the random effects for this configuration the TDOAs remain below the cyclic prefix limit defined in 3GPP/LTE. When considering random shadowing there could even occur worst case scenarios where the long CP is exceeded. In [GKF12] comparable results were also measured in an urban field trial. For inter-site distances from 450-1000 m in 20% of the transmission scenarios TDOAs larger than 2 μs have been observed which substantiates the results presented here. Thus, it can be concluded that in realistic CoMP networks the TDOAs will even become

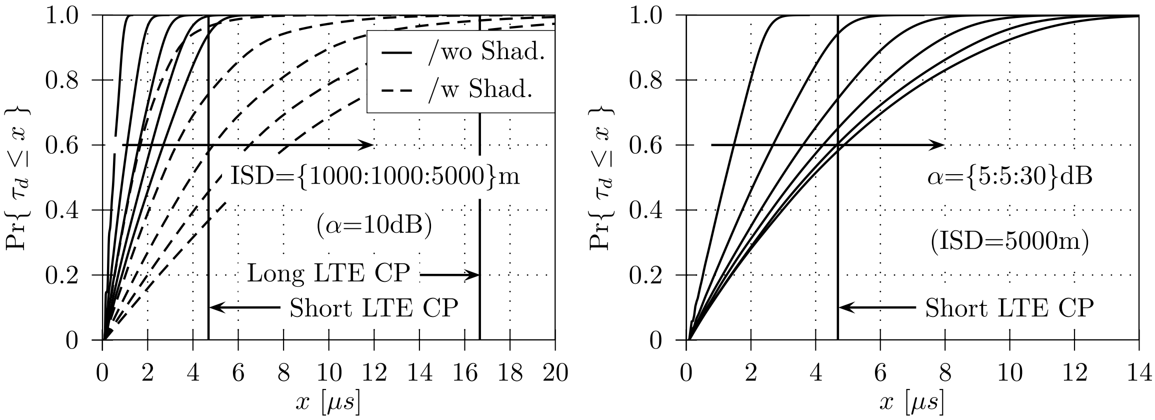

Figure 2.8.: Occurring TDOAs for different ISDs (left,solid) as well as shadow fading (left,dashed) and different cooperation ranges α (right) /wo shadow fading (Cell setup as defined in Tab. 2.1, NLOS, omni-directional antenna pattern).

critical for medium cell sizes when using the short cyclic prefix.

On the right-hand side of Fig. 2.8 the dependency of the occurring TDOAs on the cooperation range is shown, but for the sake of clarity only for a deterministic pathloss scenario. Compared to Fig. 2.4, where the link separation values are shown for the same setup, it can be observed again that for higher cooperation ranges the occurring TODAs will not increase linearly.

It should be noted that in the preceding paragraph only time asynchronisms are considered. But a similar behavior also holds for the frequency synchronization in the case that the core network is insufficiently synchronized. The main difference is that the frequency mismatches are *not* distance dependent. The impact of the occurring inter-carrier interference must then be analyzed dependent on the link separation.

Other RF Impairments: As introduced in section 2.1.2, when using OFDM the effective channel which can be observed in frequency domain also includes other impairments of the radio-frequency part of the analog as well as digital front-end of the transmitter and receiver. These impairments are not considered within the investigations throughout this thesis but for the sake of completeness they should be briefly stated here since OFDM in general is very sensitive to such impairments. A comprehensive overview as well as a complete model with important RF impairments is e.g. given in [HB08] as well as in [Sch06]. The introduced frequency offsets described above are modeled as linearly increasing phase. Real oscillators have also a noise like behavior so that the phase actually must be modeled as a random process which makes the analysis much more involved. This effect is also referred to as phase noise and is e.g. investigated in detail in [Bit09]. Due to the inaccurate local oscillator frequencies also the sampling at the ADC is not exactly equidistant as it is desired. Thus, sampling clock offsets as well as a sampling jitters could lead to performance degradations which is part of the investigations in [Löh06]. Furthermore, OFDM has in general a very high peak to average power ratio in time domain which means that the complex envelope can vary with a high dynamic. Due to the rather non-linear amplification in analog domain this could lead to a clipping of signals at high amplitude levels. The clipping is e.g. discussed in detail in [Zil07]. During the up and down conversion process it is required that the inphase as well as quadrature component are exactly shifted by 90°. This is not exactly the case in practical devices which leads to imbalanced I and Q branches. A detailed analysis for this problem can be found in [Win07].

2.3. Summary

In this chapter the basic relations of OFDM based CoMP systems have been reviewed which are necessary to proceed with a detailed analysis of the considered impairments to those systems in the following chapters. Therefore, at first in section 2.1.1 wireless channel access techniques were briefly discussed. This was in particular important for pointing out the main differences between systems with base station cooperation and existing transmission schemes. The underlying MIMO OFDM transmission model on link level has been introduced in section 2.1.2 as this is essential to investigate the impact of the time and frequency asynchronisms on the system performance in the following chapters. As it is widely known, an important fact when using OFDM is that the timing delays of the incoming propagation paths must not exceed the cyclic prefix limit in order the preserve the orthogonality among the subcarriers in frequency domain.

In section 2.2 the transition of the existing multiple antenna technology to distributed antenna systems was discussed in detail. As pointed out, the main differences between MIMO and CoMP systems on the physical layer are the distance dependent channel characteristics. Therefore, in section 2.2.1 the impact of the pathloss on the link separation among the spatially coupled users was investigated. It could be concluded that it is beneficial when grouping users and base station into a cooperation cluster that are within a defined cooperation range in which similar link SNR values are achieved. Otherwise the links are already decoupled and the joint signal processing would not lead to significant performance improvements. The network and terminal synchronization was part of the investigations in section 2.2.2. At first the main synchronization issues for point to point communications are summarized. Thereafter, the specific phenomenon of the time differences of arrival in multi-point to multi-point systems was discussed. It turned out that particularly in systems with large inter-site distances the occurring TDOAs would require a large cyclic prefix but this would also decrease the spectral efficiency. This problem even gets worse when considering stochastic pathloss models where the geographical distance between the base stations and the user terminals are not deterministically coupled anymore.

While in this chapter it was always assumed that the cyclic prefix is designed to be large enough to avoid inter-symbol interference as well as that no frequency mismatch occurs in the next chapter the impact of the asynchronous interference on the MIMO OFDM transmission model is investigated in detail.

CHAPTER 3

CHARACTERIZATION OF ASYNCHRONOUS INTERFERENCE

Throughout the previous chapter the multi-carrier multi-antenna system model has been introduced in detail. Furthermore, it turned out that the network synchronization in cooperating base station systems cannot always ensure a reliable OFDM transmission without violating the sampling theorem in frequency and time. This means that either one has to cope with such interference or one needs to avoid those coupling scenarios. Within this chapter the impact of time and frequency asynchronisms on MIMO OFDM transmission is investigated in general. Therefore in section 3.1 at first the time and frequency domain transmission model *with* time and frequency asynchronisms is derived. The focus therein is a transmission model in frequency domain that includes all considered impairments to carry out a detailed asynchronous interference analysis for the expected signal distortions on each subcarrier. This will be done in section 3.2 where also some approximations are provided, usable as rough estimates for expressing the impact of the asynchronisms e.g. in system level simulations. In section 2.2 of the previous chapter cooperating base station systems were analyzed with the focus on *avoiding* time and frequency mismatches. In section 3.2.3 similar investigations are carried out to show the system performance under the influence of *arbitrary* time and frequency asynchronisms which reflects a more realistic system behavior. The results aim at giving more insight into basic limitations as well as to provide conclusions for the parameter design when setting up a cooperating base station network.